Materials Science-Poland, 30(4), 2012, pp. 335-341
http://www.materialsscience.pwr.wroc.pl/
DOI: 10.2478/s13536-012-0057-5

Electrical properties of dielectric foil for embedded PCB capacitors*

T. PIASECKI[1†], K. NITSCH[1], A. DZIEDZIC[1], K. CHABOWSKI[1], W. STĘPLEWSKI[2], G. KOZIOŁ[2]

[1] Faculty of Microsystem Electronics and Photonics, Wrocław University of Technology, ul. Janiszewskiego 11/17, 50-372 Wrocław, Poland

[2] Tele and Radio Research Institute, ul. Ratuszowa 11, 03-450 Warszawa, Poland

One of the methods of achieving high packaging density of passive elements on the PCB is using the capacitors embedded in multilayer PCB. Test structures consisting of embedded capacitors were fabricated using the FaradFlex® capacitive internal layers. Impedance spectroscopy and equivalent circuit modelling was used to determine their electrical properties such as the capacitance, parasitic resistance and inductance. The use of several stages of accelerated ageing allowed us to test the durability of the structures. The results showed good quality stability of the embedded elements. The spatial distribution of the capacitance of the test structures on the surface of the PCB form was tested. The influence of the process parameters during lamination on the values of embedded capacitors was revealed.

Keywords: *impedance spectroscopy, equivalent circuit, dielectric foil, embedded elements, PCB*

1. Introduction

One of the methods for increasing the density of elements on the printed circuit board (PCB) and reducing the number of soldered joints is the embedding of passive elements in the internal layers of the PCB [1–3]. It allows reducing the manufacturing costs and improving the electrical properties of passive elements.

The impedance spectroscopy is a useful method for determining the electric properties of materials and electronic devices [4, 5]. It is based on measurement and analysis of the electric response of an object excited with a small electromagnetic signal in a wide range of frequency – the impedance spectrum.

The impedance spectra are most often analysed using equivalent circuit modelling. This method makes possible to identify separately the phenomena which determine the electric properties of the object as well as its parasitic elements.

In this paper, authors present the results of investigation of dielectric foil properties and their changes during accelerated ageing identified using the impedance spectroscopy.

2. Samples and measurement system

The properties of commercial FaradFlex® copper coated dielectric foils were measured using planar capacitors embedded in the PCB. Two types of foils were used: BC24M polymer foil and BC12TM foil which additionally contained the high permittivity ceramic powder. These foils had thicknesses of 24 and 12 μm, respectively and the characteristic capacitance of 180 pF/cm^2 and 650 pF/cm^2, respectively [6, 7].

Each foil was used to fabricate three test PCBs. First, the capacitor plates were etched in the FaradFlex® copper coating and the copper surface was developed in an oxidation process. Then, the structure consisting of the bottom FR4 substrate, 2 × 106 prepreg, the FaradFlex® foil, the second layer of 2 × 106 prepreg and the top FR4 was stacked and laminated at the pressure of 3 MPa and temperature

*This paper was presented at the 35th International Microelectronics and Packaging IMAPS-IEEE CPMT Poland Conference, 21–24 September 2011, Gdańsk-Sobieszewo, Poland

†E-mail: tomasz.piasecki@pwr.wroc.pl

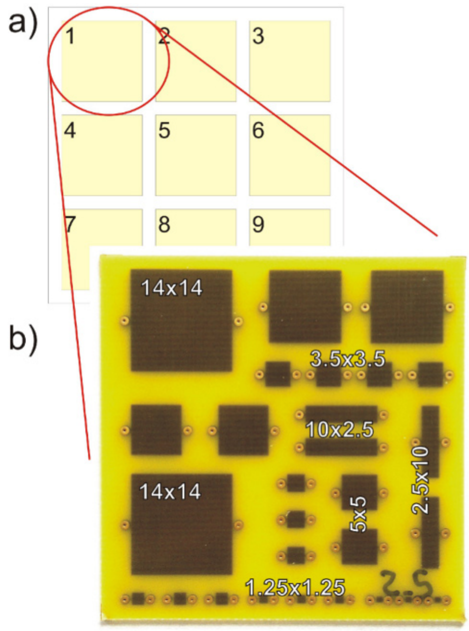

Fig. 1. The schematic of PCB board (a) and layout of one of coupons (b). Dimensions in millimetres.

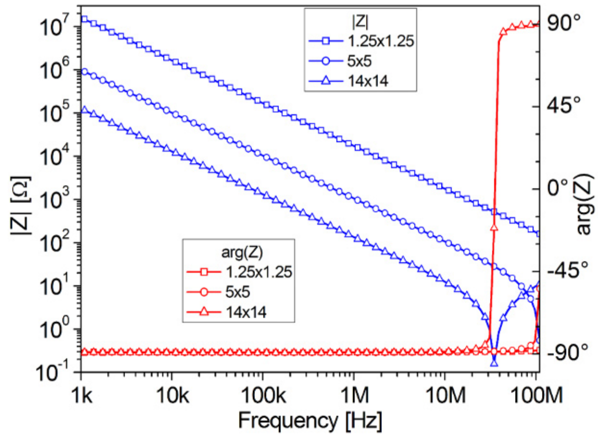

Fig. 2. Exemplary measured (dots) and fitted (line) impedance spectra of BC12TM capacitors of different sizes.

of 180 °C. Afterwards, the holes were drilled and plated and the outer copper layer was etched and gold plated to form the contacts to the embedded capacitors.

Each PCB consisted of nine identical coupons (Fig. 1a) which were then separated, however, marks on the coupons allowed us to determine their original position on the PCB.

Each coupon consisted of several test structures with different sizes. The dimensions of the test structures are shown in Fig. 1b. The 5×5, 10×2.5 and 2.5×10 structures had the same area but different aspect ratios, which might have the influence on the capacitor electric properties.

The impedance spectra were measured using Agilent 4294A impedance analyser in the frequency range of 1 kHz to 110 MHz with dedicated high-frequency electrode system. The electrode system had minimised parasitic elements ($C < 30$ fF, $L < 8$ nH, $R < 30$ mΩ) and was designed in a way allowing us to perform a complete leads compensation procedure in the impedance analyser. The measurement of impedance spectra was controlled by the home-built software, *Impedancer* [8]. The spectra were presented and analysed using Scribner ZView®. The measurements of temperature dependence were conducted on the water-cooled Peltier stage with PID temperature controller.

After the initial measurement, the coupons were divided into two batches and subjected to two different accelerated ageing processes:
Process 1: 150 h at 60 °C, 95 % RH
Process 2: 150 h at 140 °C

After the accelerated ageing processes, the test structures were measured again.

3. Results

3.1. Impedance measurements and equivalent circuit analysis

Exemplary impedance spectra of embedded capacitors, measured at room temperature, are shown in Fig. 2.

All samples exhibited capacitive character of impedance in the whole frequency range except for the largest capacitor where, in spite of using low-inductance electrodes system, the self-resonance was observed.

The plot of equivalent parallel capacitances and loss factors for similar BC12TM and BC24M samples (Fig. 3) indicated the decrease of capacitance with increasing frequency, which is well described in equivalent circuit modelling by using constant phase elements [4] in situations where electrodes

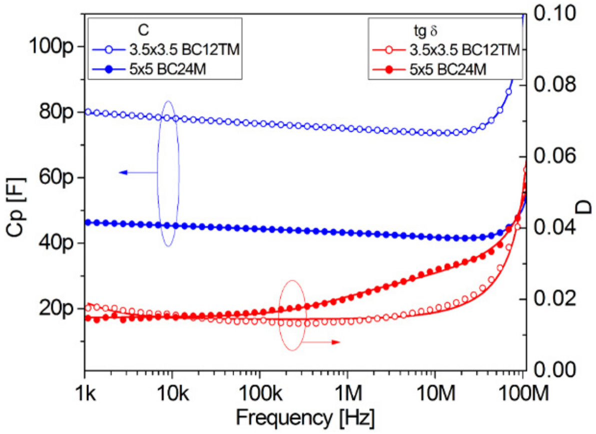

Fig. 3. Exemplary measured (dots) and fitted (line) capacitance (Cp) and loss factor (D) for BC12TM and BC24M capacitors.

roughness [9] or non-uniformity in current density [10] occur. The apparent rise of equivalent capacitance at frequencies above 20 MHz was caused by parasitic series inductance and resistance.

The average values of electric parameters of embedded elements for each type of foil and test capacitor dimensions, measured at 1 MHz, are shown in Table 1.

The measured values of capacitance density were in a good correlation with the nominal ones. Apart from the smallest test capacitors, for which the manufacturing errors play the most significant role, the measured capacitance density was by about 6 % smaller than the nominal for BT12TM and by about 2.5 % smaller for BT24M.

The loss factor was similar to the nominal only for BC12TM foil. For the BC24M, the measured loss factor was up to 40 % greater than the nominal value. The peak in the loss factor at the room-temperature impedance spectrum (Fig. 3) at around 10 MHz suggested the existence of dielectric relaxation in the measured sample. To investigate this observation, the series of impedance spectra of 3.5×3.5 mm BC12TM and 5×5 BC24M capacitors were measured in the temperature range of −20 to 110 °C. The selected results are shown in Fig. 4.

The peaks in the loss factor spectra, typical of dielectric relaxations, were observed for both samples but at different temperatures and frequencies. Equivalent circuit modelling was used to calculate the relaxation times and their dependence on the temperature. The proposed serial equivalent circuit is shown in Fig. 5 and exemplary values obtained in the fitting procedure, in Table 2.

The model consisted of two pairs of constant phase element in parallel with a resistor connected in series, used to model the Maxwell-Wagner polarization [4, 5]. The CPE together with RP modelled the dielectric properties and leakage of the dielectric foil itself while the CPE_1, characterized by the relatively big Q-parameter, and R_1 were the most probably related to the thin boundary layer at the interface between the copper electrodes and the dielectric foil. R_S and L_S modelled the parasitic series resistance and inductance. The relaxation times were calculated from the values of fitted element using serial – parallel model transformation [11], and are shown in Fig 6.

In both samples the values of calculated activation energy were similar, therefore, the complex composition of the dielectric foil itself was excluded as the cause of dielectric relaxation because only the BC12TM foil contained the powdered high-permittivity ceramics.

3.2. Electric properties of dielectric foil after the accelerated ageing

As mentioned above, the samples were measured before and after two types of accelerated ageing processes. To evaluate the tolerances and stability of the dielectric foil, the statistical analysis of capacitance and loss factor at frequency of 1 MHz for fresh and aged samples was conducted. The relative changes of capacitance and loss factor δC and δD were calculated as follows:

$$\delta C = \frac{\bar{C}_0 - \bar{C}}{\bar{C}} \tag{1}$$

$$\delta D = \frac{\bar{D}_0 - \bar{D}}{\bar{D}} \tag{2}$$

where $\bar{C}_0$, $\bar{D}_0$ and $\bar{C}$, $\bar{D}$ were mean values of fresh and aged sample capacitances and loss factors. The results of calculations are shown in Fig. 7.

Stability of the capacitance density of the tested dielectric foils was excellent. The changes caused by ageing did not exceed 1 %. The loss factor, however, changed more significantly. Its rise after the

Table 1. Measured capacitance (C) and loss factor (D) of test capacitors, calculated capacitance density (CP) and relative deviations of CP and D from the nominal values at 1 MHz [6, 7].

foil	size (mm×mm)	C (pF)	$D \cdot 10^{-2}$	CP (pF/cm^2)	δ (CP)	δ (D)
BC12TM	1.25×1.25	9.32	1.42	596.5	−8.24 %	−4.9 %
	3.5×3.5	75.0	1.35	611.8	−5.88 %	−9.8 %
	2.5×10	153	1.36	612.1	−5.83 %	−9.1 %
	5×5	151	1.32	605.7	−6.81 %	−12.2 %
	10×2.5	153	1.35	610.5	−6.08 %	−10.0 %
	14×14	1199	1.29	611.9	−5.86 %	−14.2 %
BC24M	1.25×1.25	2.85	2.10	182.4	1.33 %	40.1 %
	3.5×3.5	21.6	2.06	175.7	−2.39 %	39.5 %
	2.5×10	43.9	2.09	176.4	−2.02 %	37.5 %
	5×5	43.8	2.06	175.4	−2.58 %	37.4 %
	10×2.5	43.8	2.10	175.0	−2.76 %	39.8 %
	14×14	342	1.96	174.5	−3.07 %	30.3 %

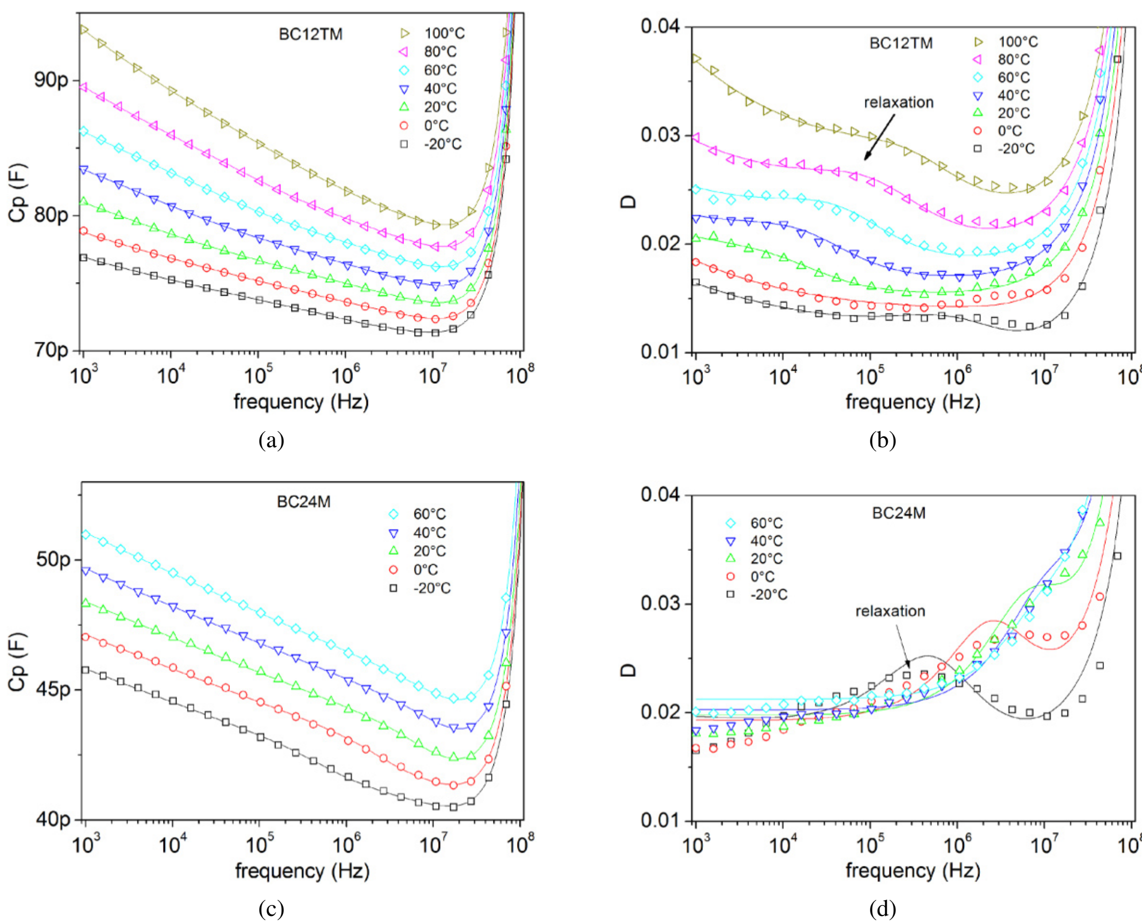

Fig. 4. Temperature dependence of measured (points) and fitted (lines) capacitance (a,c) and loss factor (b,d) spectra for 3.5 × 3.5 mm BC12TM (a,b) and 5 × 5 mm BC24M (c,d) capacitors.

Table 2. Exemplary model parameters for embedded capacitors.

sample	T	CPE-Q [Ss^n]	CPE-n	R_P [TW]	CPE1-Q [Ss^n]	CPE$_1$-n	R_1 [Ω]	R_S [Ω]	L_S [nH]
BC12TM	60 °C	$9.51 \cdot 10^{-11}$ ±1 %	0.988 ±0.1 %	0.26 ±22 %	$9.6 \cdot 10^{-9}$ ±38 %	0.96 ±5 %	1800 ±40 %	0.6±2 %	13±3 %
BC24M	0 °C	$5.2 \cdot 10^{-11}$ ±0,6 %	0.991 ±0.01 %	–	$2.6 \cdot 10^{-8}$ ±21 %	0.86 ±1.4 %	84 ±9 %	0.8 ±6 %	14 ±7 %

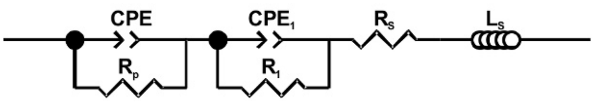

Fig. 5. Equivalent electric circuits used in the modelling.

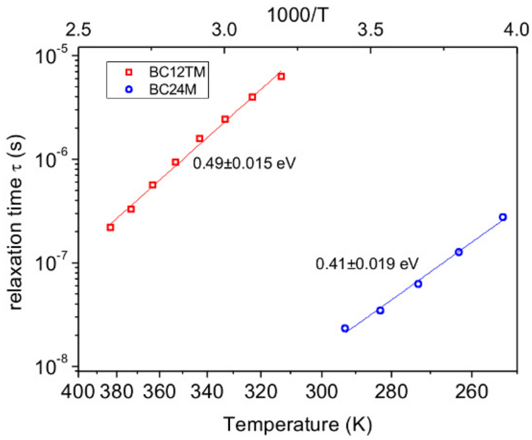

Fig. 6. Arrhenius plot of relaxation times and calculated activation energies for BC12TM and BC24M samples.

ageing process 1, which was conducted in high humidity, was probably caused by the incorporation of water in the PCB. The water content was reduced in the ageing process 2 in dry air at high temperature, causing the decrease in the loss factor values. It was impossible to determine whether these changes resulted from the changes in the dielectric foil itself or in the whole PCB.

The calculated standard deviations of capacitances were greater than the capacitance changes during ageing, exceeding 3 % for 1.25×1.25 BC12TM. To check the cause of the electric parameters variation, the spatial distribution of capacitance and loss factors were calculated.

As mentioned in Section 2, each PCB consisted of 9 coupons arranged in 3×3 grid. This allowed us to calculate the mean values of electric parameters for the capacitors on coupons which previously were at each of 9 possible locations on the PCB. The exemplary spatial distribution of capacitance and loss factor for 5×5 BC12TM sample are presented in Fig. 8 in the form of contour maps.

The patterns presented in Fig. 8 show that the distribution of the electrical properties of dielectric foil on the surface of the PCB was not random but systematic. The capacitance was greater at the left and right side of PCB and smaller at the top and centre. Similarly, the loss factor was the smallest at the centre and the greatest at the bottom of the PCB. Such behaviour was probably caused by the nonuniformity of the lamination process parameters such as the pressure or temperature. Consequently, the large difference between the minimal and maximal values of the capacitances were the main reason for the standard deviation of the calculated electrical parameters.

4. Summary

The electric properties of two types of dielectric foil (BC12TM and BC24M) were investigated by the impedance spectroscopy measurements using test structures of embedded PCB capacitors. The dielectric relaxation process was revealed, and its activation energies were similar for both types of material. Such dielectric relaxation caused a peak in the loss factor at a certain frequency and was temperature dependent.

The results of measurements after accelerated ageing revealed that the stability of the capacitance of the test structures was excellent, the changes were smaller than 1 % in comparison with the fresh samples. The loss factor however rose by about 7 % for the ageing performed in the high humidity and

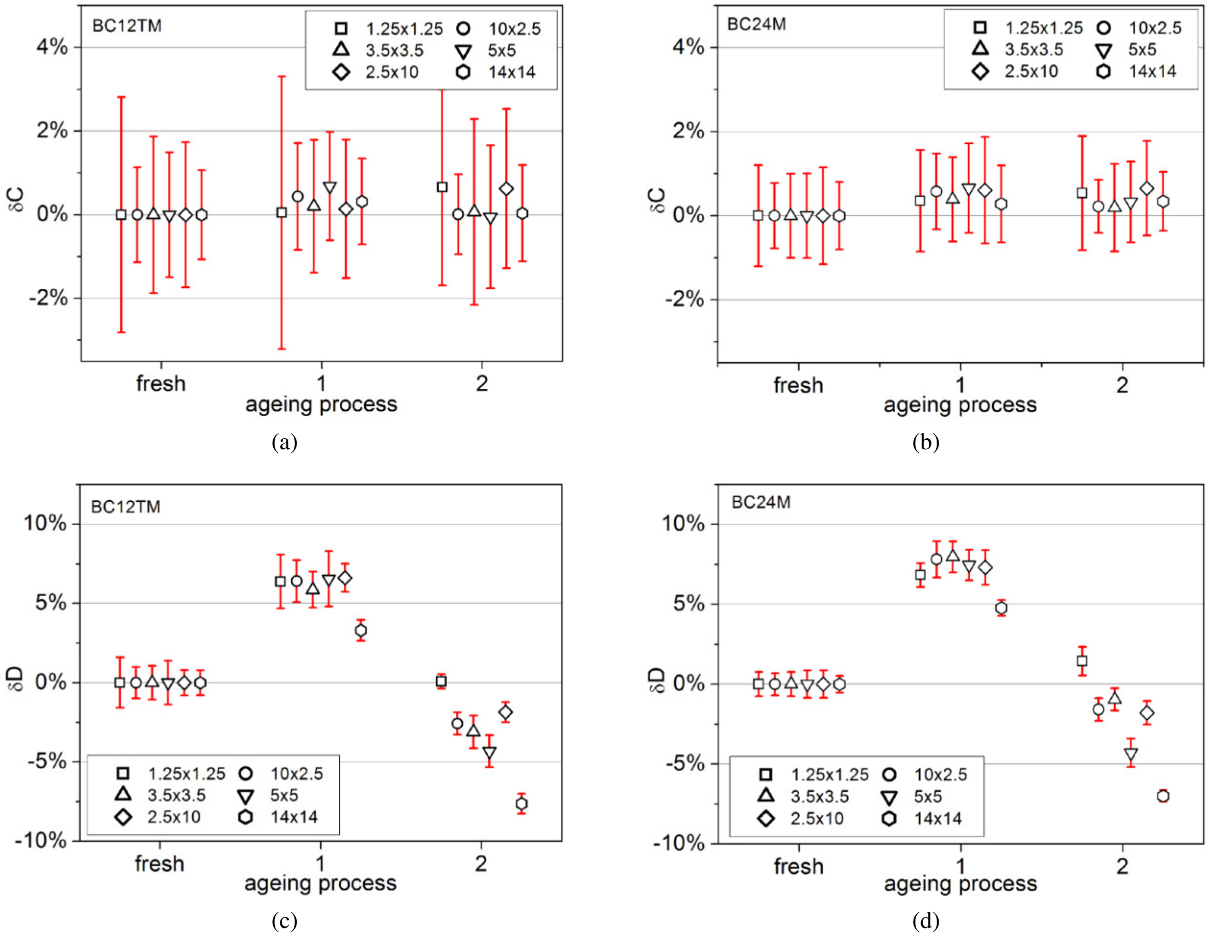

Fig. 7. Relative changes and standard deviations of capacitance (a,b) and loss factor (c,d) of fresh and aged BC12TM (a,c) and BC24M (b,d) embedded capacitors.

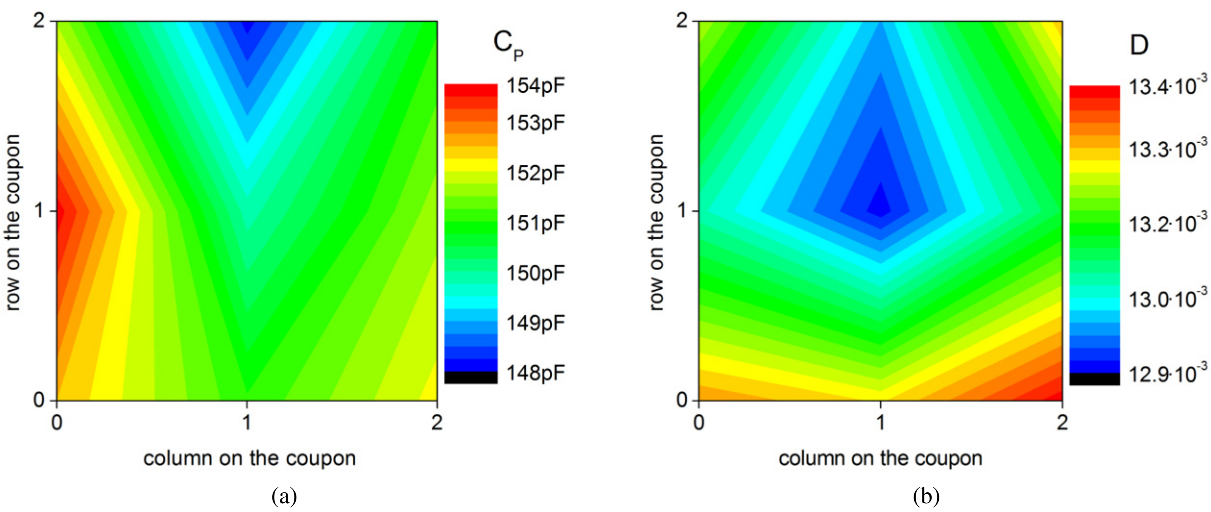

Fig. 8. Spatial distribution of mean capacitance (a) and loss factor (b) for 5×5 BC12TM sample. Rows and columns correspond to the placement of the coupon on the original PCB.

dropped by about 3–4 % for high temperature ageing process. Such changes are the result of incorporation or removing moisture from the dielectric foil.

The standard deviation of the smallest values of capacitance of the test structures reached 3 % for BC12TM and 1.5 % for BC24M foil. The analysis of spatial distribution of electrical parameters revealed that it was most probably caused by nonuniformity of the parameters during the lamination process.

Acknowledgements

Research presented in this paper was supported by Innovative Economy European Fund: "Experimental technology of embedding resistive and capacitive elements in PCB", project id: POIG.01.03.01-14-031/08 and Wrocław University of Technology statutory grant.

References

[1] DZIEDZIC A., KŁOSSOWICZ A., WINIARSKI P., NITSCH K., PIASECKI T., KOZIOŁ G., STĘPLEWSKI W., *Przegląd Elektrotechniczny*, in press.

[2] STĘPLEWSKI W., BORECKI J., KOZIOŁ G., ARAŹNA A., DZIEDZIC A., MARKOWSKI P., *Elektronika*, 52 (2011) 119.

[3] ULRICH R.K., SCHAPER L.W. (editors), *Integrated Passive Component Technology*, Wiley Interscience – IEEE Press, 2003.

[4] MACDONALD J.R., *Impedance Spectroscopy: Emphasizing Solid Materials and Systems*, John Wiley, 1987.

[5] BORSUKOV E., MACDONALD J.R., *Impedance spectroscopy. Theory, Experiment and Applications*, John Wiley, 2005.

[6] Technical datasheet: FARADFLEX® BC8TM, BC12TM, Ultra Thin Advanced Electronic Materials.

[7] Technical datasheet: FARADFLEX® BC8M, BC12M, BC16M and BC24M Ultra Thin Advanced Electronic Materials.

[8] PIASECKI T., WROŃSKI M., DUDEK M., NITSCH K., *Elektronika*, 3 (2011) 74.

[9] MULDER W.H., SLUYTERS J.H., PAJKOSSY T., NYIKOS L., *J. Electroanalytical Chemistry and Interfacial Electrochemistry*, 285 (1990) 103.

[10] JORCIN J-B., ORAZEM M.E., PEBERE N., TRIBOLLET B., *Electrochimica Acta*, 51 (2006) 1473.

[11] TADASZAK K., NITSCH K., PIASECKI T., POSADOWSKI W., *Microelectronics Reliability*, 51 (2011) 1225.

Received 2011-11-17
Accepted 2012-10-27